THE JOURNAL OF BIOLOGICAL CHEMISTRY VOL. 282, NO. 23, pp. 16783–16791, June 8, 2007

ArsD Residues Cys^{12}, Cys^{13}, and Cys^{18} Form an As(III)-binding Site Required for Arsenic Metallochaperone Activity*

Received for publication, January 30, 2007, and in revised form, March 21, 2007 Published, JBC Papers in Press, April 17, 2007, DOI 10.1074/jbc.M700886200

Yung-Feng Lin, Jianbo Yang, and Barry P. Rosen[1]

From the Department of Biochemistry and Molecular Biology, Wayne State University, School of Medicine, Detroit, Michigan 48201

The ArsA ATPase is the catalytic subunit of the ArsAB pump encoded by the *arsRDABC* operon of *Escherichia coli* plasmid R773. ArsD is a metallochaperone that delivers As(III) to ArsA, increasing its affinity for As(III), thus conferring resistance to environmental concentrations of arsenic. R773 ArsD is a homodimer with three vicinal cysteine pairs, Cys^{12}-Cys^{13}, Cys^{112}-Cys^{113}, and Cys^{119}-Cys^{120}, in each subunit. Each vicinal pair binds As(III) or Sb(III). Alignment of the primary sequence of homologues of ArsD indicates that only the first vicinal cysteine pair, Cys^{12}-Cys^{13}, and an additional cysteine, Cys^{18}, are conserved. The effect of cysteine-to-alanine substitutions and truncations were examined. By yeast two-hybrid analysis, nearly all of the ArsD mutants were able to interact with wild type ArsD, indicating that the mutations do not interfere with dimerization. ArsD mutants with alanines substituting for Cys^{112}, Cys^{113}, Cys^{119}, or Cys^{120} individually or in pairs or truncations lacking the vicinal pairs retained ability to interact with ArsA and to activate its ATPase activity. Cells expressing these mutants retained ArsD-enhanced As(III) efflux and resistance. In contrast, mutants with substitutions of conserved Cys^{12}, Cys^{13}, or Cys^{18}, individually or in pairs, were unable to activate ArsA or to enhance the activity of the ArsAB pump. We propose that ArsD residues Cys^{12}, Cys^{13}, and Cys^{18}, but not Cys^{112}, Cys^{113}, Cys^{119}, or Cys^{120}, are required for delivery of As(III) to and activation of the ArsAB pump.

Arsenic is a toxic metalloid found in water, soil, and air from both natural and anthropogenic sources. As a consequence of its environmental pervasiveness, arsenic ranks first on the United States Government's Comprehensive Environmental Response, Compensation, and Liability (Superfund) Act Priority List of Hazardous Substances (www.atsdr.cdc.gov/cercla/05list.html). Health effects associated with exposure to low levels of arsenite include cardiovascular and peripheral vascular disease, neurological disorders, diabetes mellitus, and various forms of cancer (1, 2). In response to its ubiquity in the environment, nearly every organism, from *Escherichia coli* to humans, have arsenic detoxification mechanisms (3). *E. coli* has a chromosomal three-gene *arsRBC* operon that confers moderate resistance to arsenate (As(V)), arsenite (As(III)), and antimonite (Sb(III)). However, some operons have two extra genes, a*rsD* and *arsA*, genes such as the *arsRDABC* operon in *E. coli* plasmid R773, and cells expressing the *arsRDABC* operon are more resistant to As(V) and As(III) than those expressing the *arsRBC* operon (3, 4). ArsA is a As(III)/Sb(III)-stimulated ATPase, the catalytic subunit of the ArsAB As(III)/Sb(III) extrusion pump (5). ArsD is a homodimer of two 120-residue subunits and has a weak *ars* operon repressor activity (6, 7). Recently ArsD was identified as an arsenic metallochaperone that delivers As(III) to the ArsA ATPase (4). Interaction with ArsD increases the affinity of ArsA for As(III), producing increased efflux and resistance at environmental concentrations of arsenic.

The current state of knowledge of metallochaperone-mediated ion transfer derives largely from studies of copper chaperones (8). Most copper chaperones bind copper ions with multiple cysteine ligands. In the metallochaperone CCS (copper chaperone for superoxide dismutase, four cysteine residues from both the N-terminal C*XX*C (where *X* can be any residue) motif and the C-terminal C*X*C motif form the metal-binding sites (MBSs)[2] (9). Yet only the C-terminal C*XX*C motif appears poised to deliver metal ions to the SOD1 site. Atx1 is a yeast copper chaperone that delivers copper to the transport ATPase Ccc2p in the *trans*-Golgi network (10). The human homologue of Atx1, Hah1 (Atox1), interacts with the copper-transporting ATP7A and ATP7B pumps, and mutations in these pumps lead to genetic disorders such as Menkes and Wilson diseases (11). These Atx1-like chaperones are characterized by a conserved C*XX*C motif in N terminus. However, the x-ray structure of Atx1 indicates the presence of two or even three sulfur ligands (12, 13). Two of these ligands probably derive from the C*XX*C motif, and the third could either be an exogenous thiol or a cysteine from a second Atx1 molecule. Cox17, the chaperone for cytochrome *c* oxidase, also binds copper ions with cysteine ligands. It binds three ions with a conserved CC*X*C motif in which all three cysteines are required to produce active oxidase. CopZ, characterized by a M*X*C*XX*C metal-binding motif, transfers copper ions to CopY, a copper-dependent regulatory protein (14). Copper transfer between CopZ and CopY is dependent on electrostatic interactions (15).

* This work was supported by United States Public Health Service Grant GM55425. The costs of publication of this article were defrayed in part by the payment of page charges. This article must therefore be hereby marked "*advertisement*" in accordance with 18 U.S.C. Section 1734 solely to indicate this fact.

[1] To whom correspondence should be addressed: Dept. of Biochemistry and Molecular Biology, Wayne State University, School of Medicine, Detroit, MI 48201. Tel.: 313-577-1512; Fax: 313-577-2765; E-mail: brosen@med.wayne.edu.

[2] The abbreviations used are: MBS, metal(loid)-binding site; LB, Luria broth; SD, synthetic dextrose; MBP, maltose-binding protein; dibromobimane, 4,6-bis(bromomethyl)-3,7-di-methyl-1,5-diazabicyclo[3.3.0]octa-3,6-diene-2,8-dione; MOPS, 4-morpholinepropanesulfonic acid.

TABLE 1
Strains and plasmids

Strains/plasmids	Genotype/description	Reference
***E. coli* strains**		
JM109	F' *traD36 lacIq* Δ*(lacZ)M15 proA*$^+$*B*$^+$/e14$^-$(McrA$^-$)Δ*(lac- proAB) thi gyrA96* (Nal^r) *endA1 hsdR17*(r_K^- m_K^+) *recA1 relA1 supE44*	Ref. 16
BL21(DE3)	*hsdS gal*(λc*Its857 ind1 Sam7 nin5 lac*UV5-T7 gene *l*	Ref. 16
AW3110	Δ*ars*::*cam* F$^-$ IN(*rrnD-rrnE*)	Ref. 35
***Saccharomyces cerevisiae* strain**		
AH109	*MATa, trp1-901, leu2-3, 112, ura3-52, his3-200, gal4*Δ, *gal80*Δ, *LYS2*::*GAL1*$_{UAS}$-*GAL1*$_{TATA}$-*HIS3, GAL2*$_{UAS}$-*GAL2*$_{TATA}$-*ADE2,URA3*::*MEL1*$_{UAS}$-*MEL1*$_{TATA}$-*lacZ*	Clontech
Plasmids		
pSE380	Expression vector offering *trc* promoter, *lacO* operator, *lacI*^{q} repressor (Ap^r)	Invitrogen
pMAL-c2X	A vector for expression of MBP fusion proteins (Ap^r)	New England Biolabs
pGBT9	GAL4$_{(1–147)}$ DNA-binding domain, *TRP1* (Ap^r)	Clontech
pACT2	GAL4$_{(768–881)}$ activation domain, *LEU2* (Ap^r)	Clontech
pBAD/Myc-His A	Expression vector with p_{BAD} promoter (Ap^r)	Invitrogen
pACYC184	Cloning vector (Cm^r and Tc^r)	Ref. 36
pACBAD	380-bp BclI-EcoRI fragment containing the pBAD promoter of pBAD/Myc-HisA cloned into pACYC184 (Tc^r)	Ref. 4
pACT-X series	*arsA* and *arsD* genes cloned in pACT2 (Ap^r)	Ref. 4
pSE-X series	*arsAB* or *arsB* gene in pSE380 (Ap^r)	Ref. 4
pMAL-Dx series	MBP-fused *arsD* derivatives in pMAL-c2X (Ap^r)	This study
pGBT-Dx series	*arsD* derivatives in pGBT9 (Ap^r)	This study
pACBAD-Dx series	*arsD* derivatives in pACBAD (Tc^r)	This study

By extrapolation of the role of thiol-metal ion chemistry in copper chaperones, we considered the possibility that As(III)-thiol interactions might be involved in its chaperone activity. ArsD has three vicinal cysteine pairs, Cys^{12}-Cys^{13}, Cys^{112}-Cys^{113}, and Cys^{119}-Cys^{120}. Cysteine residues 12, 13, and 18 are conserved in all known ArsD homologues. In contrast, the last two vicinal cysteine pairs are found only in some homologues (see Fig. 1). To examine the role of these cysteine residues in ArsD metallochaperone activity, a series of mutants and truncations were created. Analysis of these variants demonstrates that each of the three vicinal pairs forms an independent metalloid-binding site. The data suggest that only the As(III)-binding site formed by the CCX_4C motif is required for metallochaperone activity.

MATERIALS AND METHODS

Strains, Plasmids, and Media—Strains and plasmids used are given in Table 1. *E. coli* cells were grown in Luria-Bertani (LB) medium (16) at 37 °C. Ampicillin (100 μg/ml), tetracycline (10 μg/ml), chloramphenicol (50 μg/ml), kanamycin (40 μg/ml), and 0.3 mM isopropyl-β-D-thiogalactopyranoside were added as required. Yeast cells were grown in complete yeast extract-peptone-dextrose or minimal synthetic dextrose (SD) media (17) with the appropriate supplements at 30 °C. Growth in liquid culture was estimated from the absorbance at 600 nm.

DNA Manipulations—General molecular biological procedures were performed as described (16). Transformation of *E. coli* cells was carried out using a Bio-Rad MicroPluser. Site-directed mutagenesis was performed using a QuikChange site-directed mutagenesis kit (Stratagene, La Jolla, CA). Transformation of yeast cells was carried out using a Geno FAST-Yeast transformation kit (Geno Technologies, St. Louis, MO).

Protein Expression and Purification—Cells bearing the indicated plasmids were grown in LB medium overnight at 37 °C and then diluted 50-fold into 1 liter of the same medium. Proteins were expressed by induction with 0.3 mM isopropyl-β-D-thiogalactopyranoside at A_{600} of 0.6–0.8 for 3 h. ArsD derivatives with the maltose-binding protein (MBP) at the N terminus were purified from *E. coli* strain BL21(DE3) bearing plasmid pMAL-Dx series as described (4). ArsA with a six-histidine tag at the C terminus was purified from cells of strain BL21(DE3) expressing pSE-AB plasmid, respectively, as described (18). Proteins were stored at −80 °C until use, and the concentrations were determined according to the method of Bradford (19) or from the absorption at 280 nm (20).

Measurement of Metalloid Binding—The buffer used for purification of MBP-ArsD was exchanged with a buffer containing 50 mM MOPS-KOH, pH 7, using a Bio-Gel P-6 Micro Bio-Spin column (Bio-Rad). The buffers were degassed by bubbling with argon. Purified protein was incubated at 4 °C with indicated concentrations of Sb(III) in the form of potassium antimonyl tartrate. After 1 h, each sample was passed through a Bio-Gel P-6 column pre-exchanged with the same buffer. Portions (30 μl) were diluted with 2% HNO_3, and the quantity of metalloid was measured by inductively coupled mass spectrometry with a PerkinElmer ELAN 9000. Antimony standard solutions in the range of 0.5–10 ppb in 2% HNO3 were obtained from Ultra Scientific, Inc. (North Kingstown, RI).

Cross-linking Assays—Cross-linking with dibromobimane, which forms fluorescent adducts with two thiols that are 3–6 Å from each other, was performed as described previously (21). Purified MBP-ArsD derivatives were buffer-exchanged into 50 mM MOPS, 0.2 M NaCl, pH 7.5, using micro-spin gel filtration columns (Bio-Rad). The proteins were quantified and expressed as molar concentration of ArsD monomer. Proteins (24 μM each) were incubated with 0.5 mM dibromobimane for 20 min at room temperature. The samples were analyzed by 8% SDS-PAGE. Formation of fluorescent cross-linked products was visualized at 365 nm and by immunoblotting with antiserum against ArsD.

ATPase Assays—ATPase activity was estimated using a couple assay (22), as described (23). MBP-ArsD derivatives were added at a final concentration of 3 μM into an assay mixture

containing 5 mM ATP, 1.25 mM phosphoenolpyruvate, 0.25 mM NADH, 10 units of pyruvate kinase and lactate dehydrogenase with or without various concentrations of potassium antimonyl tartrate or sodium arsenite. ArsA was added to a final concentration of 0.3 μM. The mixture was prewarmed to 37 °C, and the reaction was initiated by the addition of 2.5 mM $MgCl_2$ and measured at 340 nm. The linear steady state rate of ATP hydrolysis was used to calculate specific activity. The reaction volume was 0.2 ml each in 96-well microplates, and the reactions were monitored by microplate reader SPECTRA max 340PC (Molecular Devices).

Yeast Two-hybrid Analysis—A GAL4-based yeast two-hybrid system (24) (Clontech Laboratories, Inc.) was used to determine protein-protein interactions. AH109, a GAL4-activating *HIS3* reporter yeast strain, was co-transformed with *ars* gene-fused pGBT-Dx (BD-ArsDx) and pACT-X (AD-X) series plasmids. The transformed cells were cultured overnight in SD medium at 30 °C and then washed, suspended, and adjusted to an absorbance at 600 nm of 1 in 20 mM Tris-HCl, pH 7.5. Portions of the cell suspensions (1 μl) were inoculated on SD agar plates lacking histidine in serial 10-fold dilutions and incubated at 30 °C for 3 days.

Transport Assays—Transport of As(III) by the ArsB pump was assayed as decreased accumulation in cells (25, 26), *E. coli* strain AW3110 was co-transformed with pSE-X series and pACBAD-Dx series plasmids. The cultures were grown overnight in LB medium and diluted 50-fold into LB medium at 37 °C. After 1 h 0.05% arabinose was added to induce ArsD expression, and the cells were harvested at an A_{600} of 1. The cells were washed and suspended in 1/10 of the original volume in a buffer consisting of 75 mM HEPES-KOH, 0.15 M KCl, and 1 mM $MgSO_4$, pH 7.5, 22 °C. Transport assays were performed with 10 μM sodium arsenite. Arsenic was determined by inductively coupled mass spectrometry with a PerkinElmer ELAN 9000. Protein expression levels were determined by immunoblotting using anti-ArsA and anti-ArsD antibodies.

Resistance Assays—E. coli strain AW3110 cells harboring pSE-X series and pACBAD-Dx series plasmids were grown in LB medium overnight and diluted 50-fold into LB medium containing 0.05% arabinose and various concentrations of sodium arsenite, and the absorbance at 600 nm was monitored by microplate reader SPECTRA max 340PC (Molecular Devices) with a path length of 0.24 cm at 37 °C.

RESULTS

Contribution of Cysteine Residues to ArsD Metalloid-binding Sites—Alignment of the primary sequence of homologues of R773 ArsD indicates that they all possess a vicinal cysteine pair, Cys^{12}-Cys^{13}, and a single additional cysteine, Cys^{18} (Fig. 1). Two other vicinal cysteine pairs, Cys^{112}-Cys^{113} and Cys^{119}-Cys^{120}, are found in some homologues but not others. Cys^{119}-Cys^{120} is not required for derepression by As(III) when ArsD functions as a weak transcriptional repressor, although the other two vicinal pairs may be (7, 27).

Binding of Sb(III) to purified MBP-ArsD derivatives was measured as a function of Sb(III) concentration. Sb(III) was used because it binds with higher affinity than As(III), which is difficult to measure using this assay. MBP-fused wild type ArsD bound metalloid with a stoichiometry of six Sb(III) per dimer and an apparent K_d of 10^{-6} M (Fig. 2*A*), suggesting that there are three metalloid-binding sites (MBSs) per ArsD monomer. Given the insensitivity of the assay, the actual K_d values could be lower. An ArsD derivative, $ArsD_{1-118}$, in which Cys^{119} and Cys^{120} were replaced with a six-histidine tag, bound four Sb(III) per dimer, consistent with the C-terminal vicinal pair, Cys^{119}-Cys^{120}, forming two metalloid-binding sites (termed MBS3) per dimer. The truncation $ArsD_{1-109}$, in which a stop codon was added after the codon for residue 109, leaving only the first cysteine pair, Cys^{12}-Cys^{13}, bound two Sb(III) per dimer. This N-terminal vicinal pair is termed MBS1. A derivative, $ArsD_{1-118,C12A/C13A}$, was constructed with the N-terminal cysteine pair changed to alanines and the C-terminal vicinal pair replaced with a six-histidine tag, leaving only the second vicinal pair, Cys^{112}-Cys^{113}. This derivative bound two Sb(III) per dimer; for this reason Cys^{112}-Cys^{113} was designated MBS2. These results demonstrate that each MBS binds one atom of trivalent metalloid, for a total of three per monomer and six per dimer.

Considering that cysteine pair Cys^{12}-Cys^{13} and Cys^{18} are conserved in all ArsD homologues identified to date, three derivatives were constructed: $ArsD_{1-109,C12A}$, $ArsD_{1-109,C13A}$, and $ArsD_{1-109,C18A}$. Each variant lacked MBS2 and MBS3 and retained only two of the three conserved cysteine residues. None of the three purified proteins was able to bind Sb(III), suggesting that Cys^{18}, in addition to Cys^{12} and Cys^{13}, may be involved in the formation of MBS1 (Fig. 2*B*). Although each protein was produced in normal amounts and was fully soluble, the possibility of misfolding cannot be eliminated.

MBS1 Is Involved in Metalloid Transfer and ArsA Activation—ArsD increases the affinity of the ArsA ATPase for As(III) (4). The ability of ArsD derivatives to activate ArsA was examined (Fig. 3). In the presence of $ArsD_{1-118}$, a truncated ArsD lacking Cys^{119}-Cys^{120}, the half-maximal concentration of As(III) was 10 μM (Fig. 3*A*), similar to that of wild type ArsD (4). In the presence of $ArsD_{1-109}$, a truncated ArsD lacking both the Cys^{112}-Cys^{113} and Cys^{119}-Cys^{120} vicinal pairs, the half-maximal concentration of As(III) was 25 μM. These data suggest that neither MBS2 nor MBS3 is required for ArsD to activate ArsA. In contrast, an ArsD derivative lacking MBS1, $ArsD_{1-118,C12A/C13A}$, was not able to activate ArsA. In the presence of this derivative, the concentration of As(III) required for half-maximal stimulation of ATPase activity was 1.5 mM, similar to that of ArsA in the absence of ArsD. These data are consistent with participation of MBS1, but not MBS2 or MBS3, in increasing the affinity of ArsA for metalloid.

The effects of single cysteine substitutions in MBS1 on the ability of ArsD to activate ArsA were examined (Fig. 3*B*). Derivatives $ArsD_{1-118,C12A}$, $ArsD_{1-118,C13A}$, and $ArsD_{1-118,C18A}$, each having a cysteine-to-alanine substitution in MBS1 but retaining MBS2, were unable to activate ArsA. Cysteine-to-serine substitutions gave similar results (data not shown). Because metalloids alone augment the ATPase activity of ArsA, it seems plausible that Cys^{12}, Cys^{13}, and Cys^{18} are directly responsible for delivering As(III) to ArsA to enhance its affinity. In other words, the affinity for As(III) in the ArsD-ArsA complex would be largely determined by ArsD rather than by ArsA.

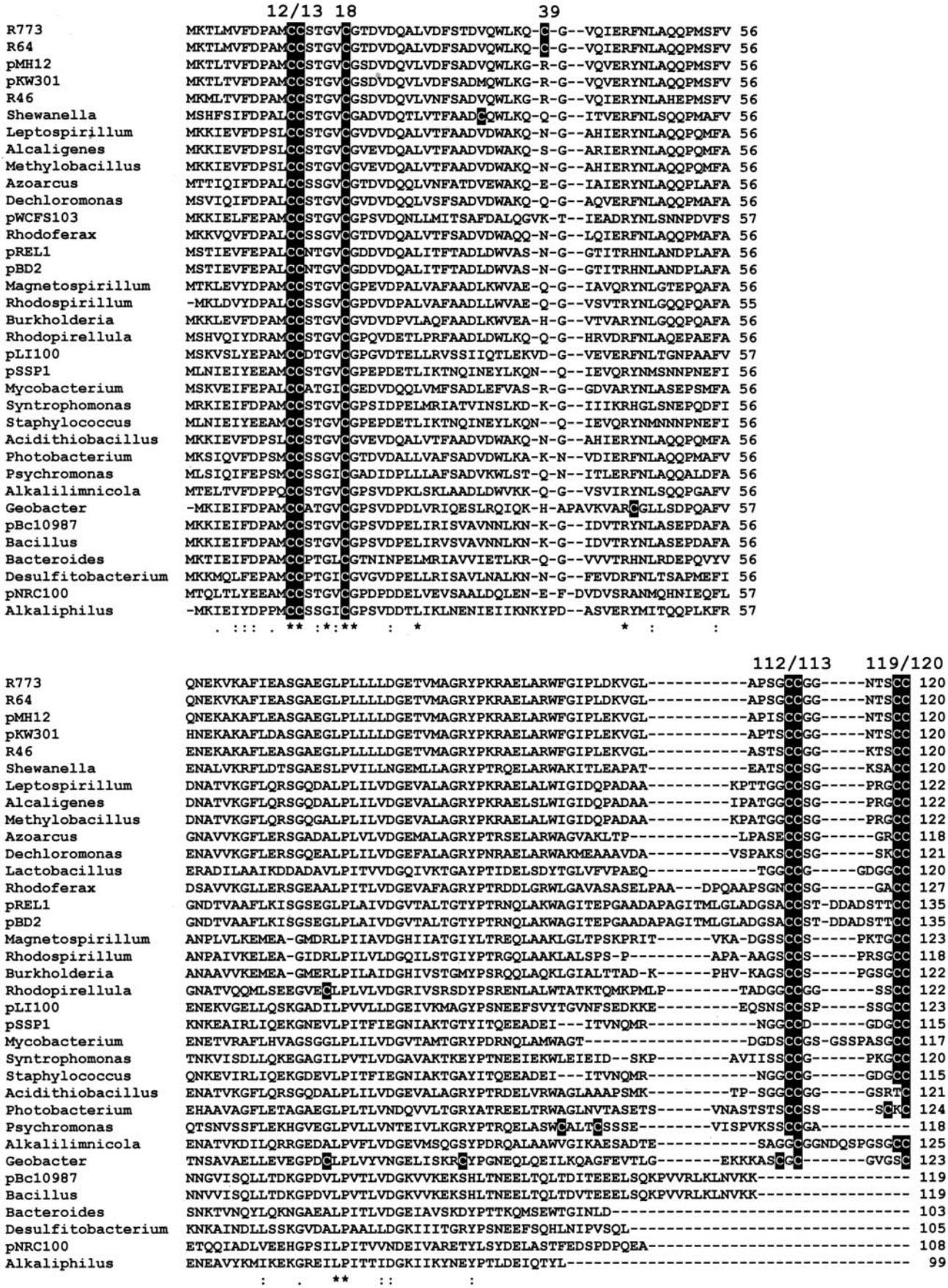

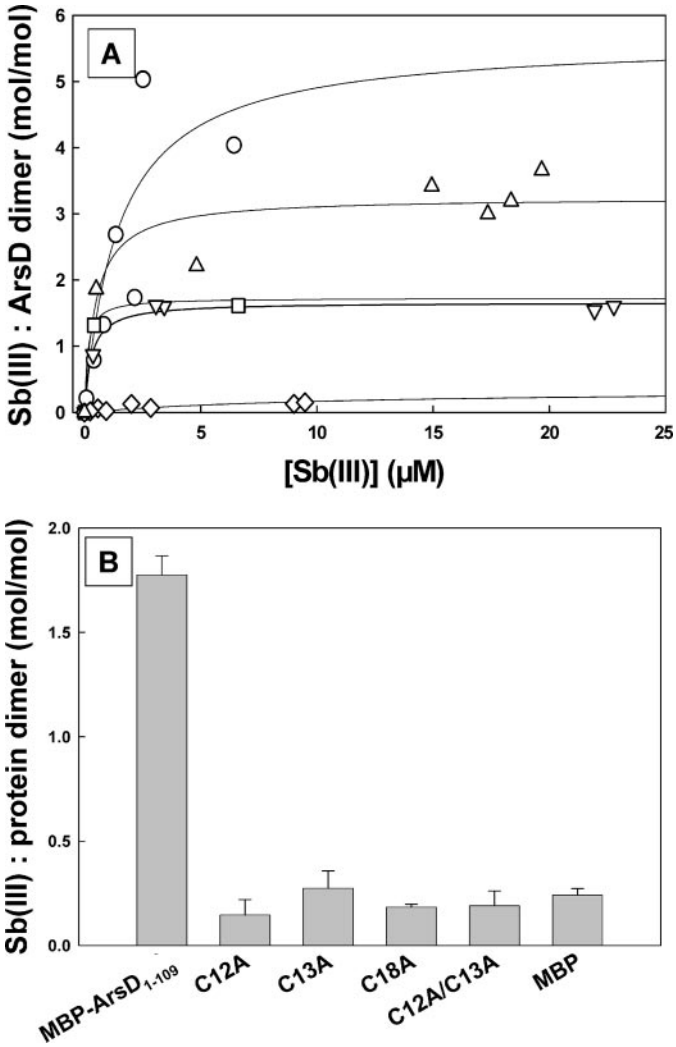

FIGURE 2. **Metalloid-binding sites in ArsD.** Purified MBP-ArsD was incubated at 4 °C with the indicated concentrations of potassium antimonyl tartrate. Sb(III)-protein complexes were obtained as described under "Materials and Methods," and the molar ratios were calculated. *A*, ArsD has three MBSs. Sb(III) binding was assayed with wild type ArsD, which has Cys^{12}-Cys^{13} (MBS1), Cys^{112}-Cys^{113} (MBS2), and Cys^{119}-Cys^{120} (MBS3) (B_{max} = 5.6 mol Sb(III)/mol ArsD dimer, K_d = 1.5 μM) (○), $ArsD_{1-118}$, which has MBS1 and MBS2 (B_{max} = 3.3 mol Sb(III)/mol ArsD dimer, K_d = 0.5 μM) (△), $ArsD_{1-109}$, which has only MBS1 (B_{max} = 1.7 mol Sb(III)/mol ArsD dimer, K_d = 0.3 μM) (▽) and $ArsD_{1-118,C12A/C13A}$, which has only MBS2 (B_{max} = 1.7 mol Sb(III)/mol ArsD dimer, K_d = 0.1 μM) (□). Maltose-binding protein was used as a control (◇). *B*, contributions of the three conserved cysteine residues to MBS1. Sb(III) binding was assayed with $ArsD_{1-109}$, which has MBS1 residues Cys^{12}, Cys^{13}, and Cys^{18}; $ArsD_{1-109,C12A}$, which has MBS1 residues Cys^{13} and Cys^{18}; $ArsD_{1-109,C13A}$, which has MBS1 residues Cys^{12} and Cys^{18}; $ArsD_{1-109,C18A}$, which has MBS1 residues Cys^{12} and Cys^{13}; $ArsD_{1-109,C12A/C13A}$, which has only MBS1 residue Cys^{18}. Maltose-binding protein was used as a control. The *error bars* represent the standard error.

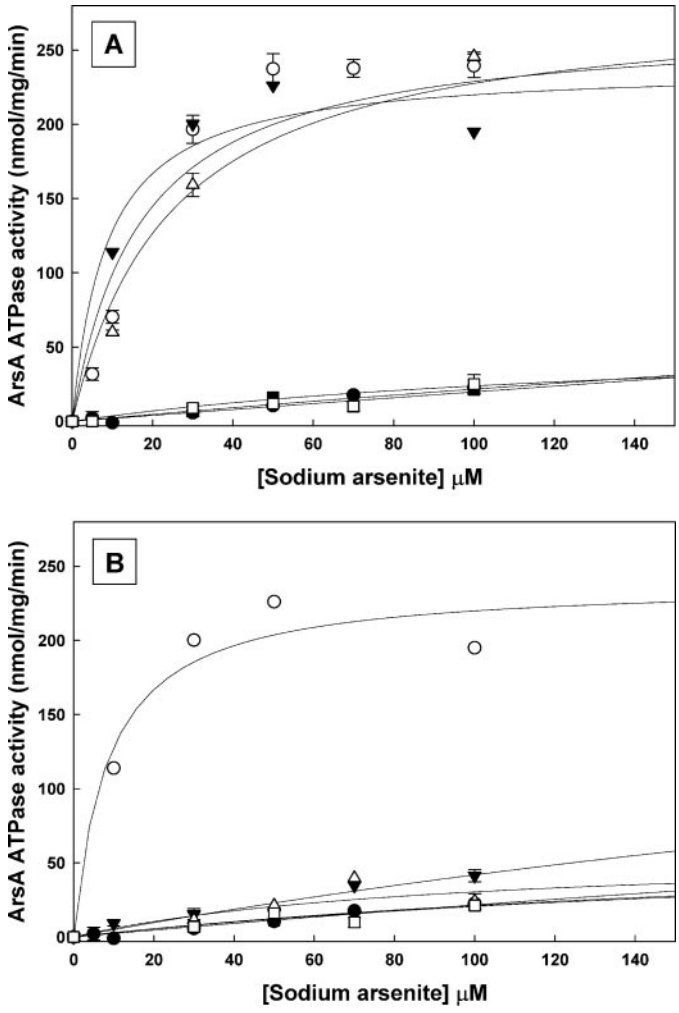

FIGURE 3. **ArsD MBSs and activation of ArsA ATPase activity.** ArsA ATPase activity was assayed at the indicated concentrations of sodium arsenite in the presence or absence of ArsD derivatives. *A*, activation of ArsA with MBS derivatives. ArsA ATPase activity was assayed as described under "Materials and Methods." ●, no ArsD; ○, wild type ArsD; ▼, $ArsD_{1-118}$ (MBS1 and MBS2); △, $ArsD_{1-109}$ (MBS1); ■, $ArsD_{1-118,C12A/C13A}$, (MBS2); □, maltose-binding protein. *B*, effect of cysteine substitutions in MBS1 on activation of ArsA. MBS2 in these ArsD derivatives were present. ●, no ArsD; ○, $ArsD_{1-118}$ (Cys^{12}, Cys^{13}, and Cys^{18}); ▼, $ArsD_{1-118,C12A}$ (MBS1 residues Cys^{13} and Cys^{18}); △, $ArsD_{1-118,C13A}$ (MBS1 residues Cys^{12} and Cys^{18}); ■, $ArsD_{1-118,C18A}$ (MBS1 residues Cys^{12} and Cys^{13}); □, $ArsD_{1-118,C12A/C13A}$ (MBS1 residue Cys^{18}). The *curves* were fitted using SigmaPlot 9.0, with the *error bars* representing the standard error.

The Effect of Elimination of ArsD As(III)-binding Sites and Truncations on Protein-Protein Interactions—The ability of the six cysteine-to-alanine ArsD mutants and two truncated derivatives to dimerize was examined by yeast two-hybrid analysis

FIGURE 1. **Multiple alignment of ArsD homologues.** Representative ArsD homologues (accession numbers in parentheses) are from: *E. coli* plasmid R773 (U13073); *Salmonella typhimurium* plasmid R64 (AP005147); *Klebsiella oxytoca* plasmid pMH12 (AF168737); *Acidiphilium multivorum* plasmid pKW301 (AB004659); *E. coli* plasmid R46 (AY046276); *Shewanella putrefaciens* CN-32 (AALB01000006); *Leptospirillum ferriphilum* transposon TnLfArs (DQ057986); *Alcaligenes faecalis* NCIB 8687 (AY297781); *Methylobacillus flagellatus* KT (CP000284); *Azoarcus* sp. EbN1 (CR555306); *Dechloromonas aromatica* RCB (CP000089); *Lactobacillus plantarum* plasmid pWCFS103 (CR377166); *Rhodoferax ferrireducens* T118 (CP000267); *Rhodococcus erythropolis* PR4 plasmid pREL1 (AP008931); *Rhodococcus erythropolis* plasmid pBD2 (AY223810); *Magnetospirillum magneticum* AMB-1 (AP007255); *Rhodospirillum rubrum* (CP000230); *Burkholderia vietnamiensis* G4 (AAEH02000012); *Rhodopirellula baltica* SH 1 (BX294149); *Listeria innocua* plasmid pLI100 (AL592102); *Staphylococcus saprophyticus* plasmid pSSP1 (AP008935); *Mycobacterium flavescens PYR*-GCK (AAPA01000005); *Syntrophomonas wolfei* (AAJG01000050); *Staphylococcus epidermidis* RP62A (CP000029); *Acidithiobacillus caldus* transposon TnAtcArs (AY821803); *Photobacterium profundum* 3TCK (AAPH01000002); *Psychromonas sp.* CNPT3 (AAPG01000022); *Alkalilimnicola ehrlichei* MLHE-1 (AALK01000009); *Geobacter uraniumreducens* Rf4 (AAON01000041); *Bacillus cereus* plasmid pBc10987 (AE017195); *Bacillus sp. CDB3* (AF178758); *Bacteroides thetaiotaomicron* VPI-5482 (AE015928); *Desulfitobacterium hafniense* Y51 (AP008230); *Halobacterium* sp. NRC-1 megaplasmid pNRC100 (AF016485); and *Alkaliphilus metalliredigenes* QYMF (AAKU01000003). The cysteine residues are indicated. The multiple alignment was calculated with CLUSTAL W (36).

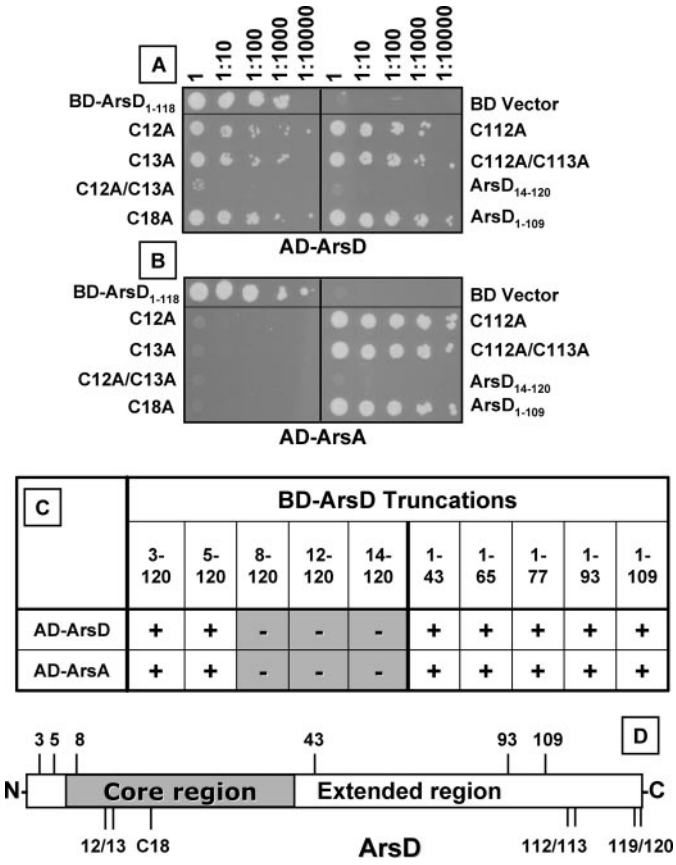

FIGURE 4. **Effect of ArsD MBS1 mutations on ArsD dimerization and interaction with ArsA.** Yeast two-hybrid analysis was performed as described under "Materials and Methods." *S. cerevisiae* strain AH109 bearing both GAL4 activation domain and binding domain (*BD*) fusion plasmids was grown in SD medium overnight and inoculated on agar plates with SD lacking histidine with 10-fold serial dilutions. As a negative control, vector plasmid pGBT9 was expressed with pACT2. *A*, ArsD dimerization. The codons for residues Cys^{12}, Cys^{13}, Cys^{18}, Cys^{112}, and Cys^{113} in $arsD_{1-118}$ were changed individually or in pairs to alanines or deleted by the indicated truncations. In each case, the altered *arsD* genes were expressed as binding domain fusions in *trans* with an activation domain fusion with a wild type *arsD* gene and allowed to grow for 3 days. *B*, ArsD-ArsA interaction. The same *arsD* constructs as above were expressed with an activation domain fusion with a wild type *arsA* gene. *C*, effects of ArsD truncations on dimerization and ArsD-ArsA interaction. The codons for the first 2, 5, 7, 11, or 13, or for the last 11, 27, 43, 55, or 77 residues were deleted. Binding domain fusions with truncated *arsD* genes were expressed *in trans* with activation domain fusions with either a wild type *arsD* or *arsA* gene. The results were expressed as growth (+) or no growth (−) after 3 days. *D*, diagrammatic representation of the ArsD monomer. The model indicates an extended region of ArsD, defined by residues that could be deleted without loss of interaction with ArsA (*open*), and a core region, defined by deletions that eliminate interactions with ArsA (*shaded*). The *upper numbers* indicate the residues remaining in the deletions. The *lower numbers* indicate the location of cysteine residues.

(see Fig. 5*A*). All of the mutants and the C-terminal truncation $ArsD_{1-109}$, which lacks the last 11 residues, were able to interact with wild type ArsD, indicating that these derivatives are stably produced in yeast and able to form dimers. Although the interaction with the mutant C12A/C13A ArsD seemed somewhat weaker than the others, yeast two-hybrid results are not necessarily quantitative. The truncated derivative lacking the first 13 residues ($ArsD_{14-120}$) was unable to interact with wild type ArsD, suggesting the involvement of those residues either in ArsD dimerization or protein stability.

The effect of the loss of MBS1, MBS2, or MBS3 on ArsD-ArsA interactions was also examined (Fig. 4*B*). The ability of three ArsD derivatives retaining MBS1 but lacking MBS2 and MBS3 was analyzed: $ArsD_{1-109}$, in which both MBS2 and MBS3 were deleted; $ArsD_{1-118,C112A}$, lacking MBS3 and one cysteine residue in MBS2 and$ArsD_{1-118,C112A/C113A,}$ lacking MBS3; and both cysteine residues in MBS2. All three mutants were able to interact with ArsA. In contrast, mutants or truncations lacking Cys^{12}, Cys^{13}, and/or Cys^{18} were unable to interact, including $ArsD_{1-118,C12A}$, $ArsD_{1-118,C13A}$, $ArsD_{1-118,C18A}$, $ArsD_{1-118,C12A/C13A}$, and a truncated derivative lacking the first 13 residues ($ArsD_{14-120}$). Cysteine-to-serine substitutions in MBS1 showed similar results as the cysteine-to-alanine substitutions (data not shown). Although it is possible that the loss of interaction is a result of misfolding, it seems unlikely that the loss in every one of these derivates could be due to misfolding, and it is more reasonable to conclude that it is due to a loss of interaction. When 0.1 mM sodium arsenite was added to the medium, the yeast cells grew more slowly, but the overall results were similar to those without metalloids (data not shown). These results suggest that cysteine residues 12, 13, and 18 are involved in interaction with ArsA.

Further truncations of ArsD that lack the first 2, 4, 7, or 11 residues or the last 27, 43, 55, or 77 residues were constructed to establish which regions of ArsD are responsible for dimerization or interaction with ArsA. The truncations were examined for ability to interact with wild type ArsD by yeast two-hybrid analysis. C-terminally truncated ArsD derivatives with as few as 43 N-terminal residues ($ArsD_{1-109}$, $ArsD_{1-93}$, $ArsD_{1-77}$, $ArsD_{1-65}$, and $ArsD_{1-43}$) were able to interact with both wild type ArsD and ArsA (see Fig. 6*C*). In contrast, truncated ArsD derivatives lacking 7 or more residues from the N terminus ($ArsD_{8-120}$, $ArsD_{12-120}$, and $ArsD_{14-120}$) were unable to interact either with wild type ArsD or with ArsA, indicating the involvement of the N terminus of ArsD in protein-protein interaction. These data are consistent with our previous suggestion that the ArsD dimer interacts with ArsA (4).

Effect of Elimination of ArsD As(III)-binding Sites on Arsenic Accumulation and Resistance—The ability of ArsD derivatives with cysteine-to-alanine substitutions to enhance the activity of the ArsAB pump *in vivo* was examined. Although cells expressing $arsD_{1-118,C112A/C113A}$, which encodes an ArsD derivative having only MBS1, *in trans* with *arsAB* accumulated As(III) to nearly the same extent as those expressing wild type *arsDAB*, cells expressing mutants lacking MBS1 ($arsD_{C12A/C13A}$ or $arsD_{C18A}$) *in trans* with *arsAB* accumulated slightly more As(III) than cells with only *arsAB* (Fig. 5*A*). These data are consistent with our proposal that Cys^{12}, Cys^{13}, and Cys^{18} are involved in functional interaction of ArsD with the ArsAB efflux pump.

We also examined whether the same *arsD* mutants affected resistance conferred by the ArsAB pump. Cells expressing an ArsD mutant having only MBS1 ($arsD_{1-118,C112A/C113A}$) *in trans* with *arsAB* had only a modest reduction in arsenite resistance compared with cells expressing wild type *arsDAB*. In contrast, cells expressing the mutants lacking MBS1 ($arsD_{C12A/C13A}$ or $arsD_{C18A}$) were no more resistant than cells with only *arsAB* (Fig. 5*B*). These results strongly support our hypothesis that the MBS1, including the Cys^{12}-Cys^{13} pair and Cys^{18}, but not MBS2 or MBS3, is required for activation of the ArsAB pump.

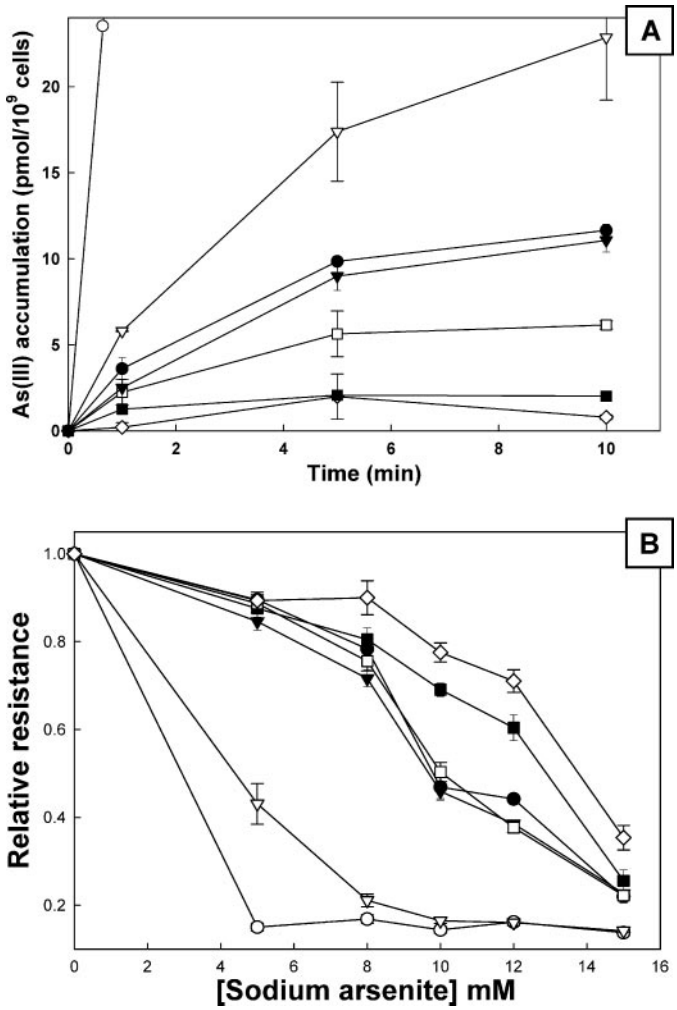

FIGURE 5. **The relationship of ArsD MBSs to arsenic accumulation and resistance.** *E. coli* strain AW3110 (Δ*arsRBC*) bearing compatible plasmids with either *arsAB* or *arsB* (in plasmid pSE380) and *arsD* (in plasmid pACBAD) genes were examined for their ability to accumulate As(III) or to grow in the presence of arsenite. *A*, As(III) accumulation. Transport assays were performed with 10 μM sodium arsenite, as described under "Materials and Methods." *B*, As(III) resistance. Resistance assays were performed at the indicated concentrations of sodium arsenite after 12 h of growth, as described under "Materials and Methods." The cells had plasmids with the following *ars* genes: ○, vector plasmids pSE380 and pACBAD; ▽, *arsB*; □, *arsAB*; ◇, *arsDAB*; ●, $arsD_{C12A/C13A}AB$; ▼, $arsD_{C18A}AB$; and ■, $arsD_{1-118,C112A/C113A}$. Each point represents the mean of three independent assays calculated using SigmaPlot 9.0 The *error bars* represent the standard error.

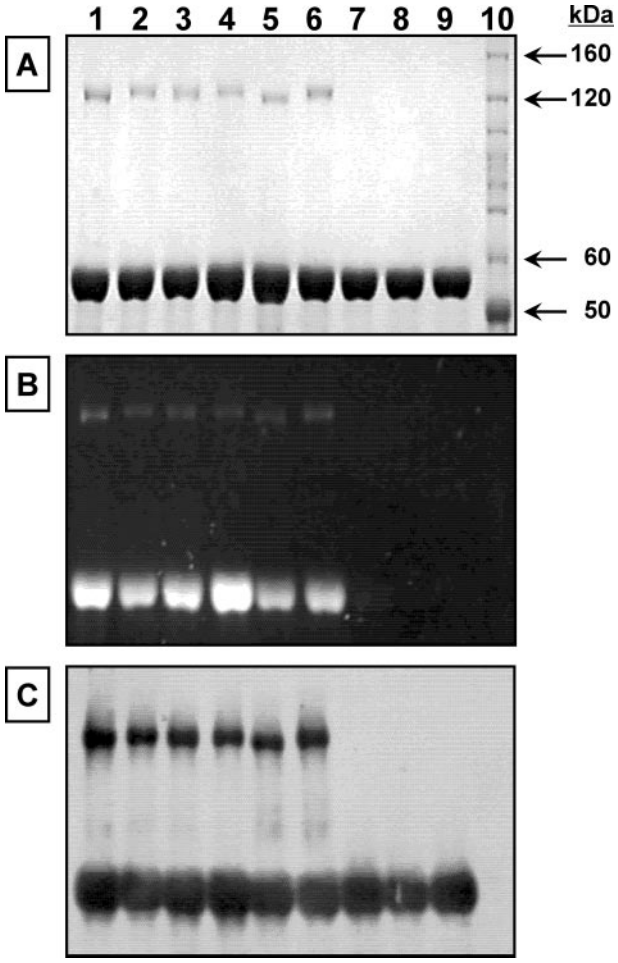

FIGURE 6. **Dibromobimane cross-linking of ArsD derivatives.** Cross-linking assays were performed as described under "Materials and Methods." MBP-ArsD chimerae (24 μM) were incubated with 0.5 mM dibromobimane at room temperature for 20 min. The samples were analyzed by SDS-PAGE on 8% polyacrylamide gels. *A*, Coomassie Blue staining. *B*, dibromobimane fluorescence. *C*, immunoblotting with anti-ArsD serum. *Lane 1*, $ArsD_{1-109}$; *lane 2*, $ArsD_{1-109,C12A}$; *lane 3*, $ArsD_{1-109,C13A}$; *lane 4*, $ArsD_{1-109,C18A}$; *lane 5*, $ArsD_{1-109,C12A/C13A}$; *lane 6*, $ArsD_{1-109,C13A/C18A}$; *lane 7*, $ArsD_{1-109,C12A/C13A/C18A}$; *lane 8*, $ArsD_{1-109}$ without dibromobimane; *lane 9*, $ArsD_{1-109,C12A/C13A/C18A}$ without dibromobimane; *lane 10*, protein standards, with masses of selected ones indicated.

ArsD Cys^{12}, Cys^{13}, and Cys^{18} in MBS1 Are Cross-linked by Dibromobimane—The proximity of three cysteine thiolates in MBS1 was examined by reaction of MBP-ArsD with the homobifunctional fluorogenic cross-linking reagent dibromobimane (Fig. 6). As expected, MBP-$ArsD_{1-109,C12A/C13A/C18A}$, lacking all three MBSs, did not react with dibromobimane (Fig. 6, *lane 7*). MBP-$ArsD_{1-109}$, having MBS1, formed a highly fluorescent monomer band and a small amount of cross-linked dimer (Fig. 6, *lane 1*). Fluorescence in the monomer band could be due in part to formation of cross-links between cysteine residues and in part to a slow, nonspecific displacement of the second bromine by water following reaction of the first with cysteine. The cross-linked dimer could form only by reaction of one cysteine in each monomers with a dibromobimane molecule. If only one cysteine residue in MBS1 was changed to an alanine, those derivatives (MBP-$ArsD_{1-109,C12A}$, MBP-$ArsD_{1-109,C13A}$, and MBP-$ArsD_{1-109,C18A}$) still formed a small amount dimer (Fig. 6, *lanes 2–4*). A derivative with only Cys^{12} (MBP-$ArsD_{1-109,C13A/C18A}$) formed fluorescent dimers with dibromobimane (Fig. 6, *lane 6*). Similarly, MBP-$ArsD_{1-109,C12A/C13A}$ (containing only Cys^{18}) formed fluorescent dimers (Fig. 6, *lanes 5*). These results suggest that the thiol groups of Cys^{12}, Cys^{13}, and Cys^{18} are probably 3–6 Å of each other in each monomer and perhaps also near the corresponding cysteine thiolates from the other subunit.

DISCUSSION

Understanding the organization of the metalloid-binding sites in the ArsD metallochaperone is crucial to a molecular description of the metalloid transfer process. Previous studies suggested from the results of indirect assays that the three vicinal cysteine pairs in ArsD form three independent metalloid-binding sites, MBS1, MBS2, and MBS3, per monomer (27, 28). In this study, binding of Sb(III) or As(III) to ArsD was directly

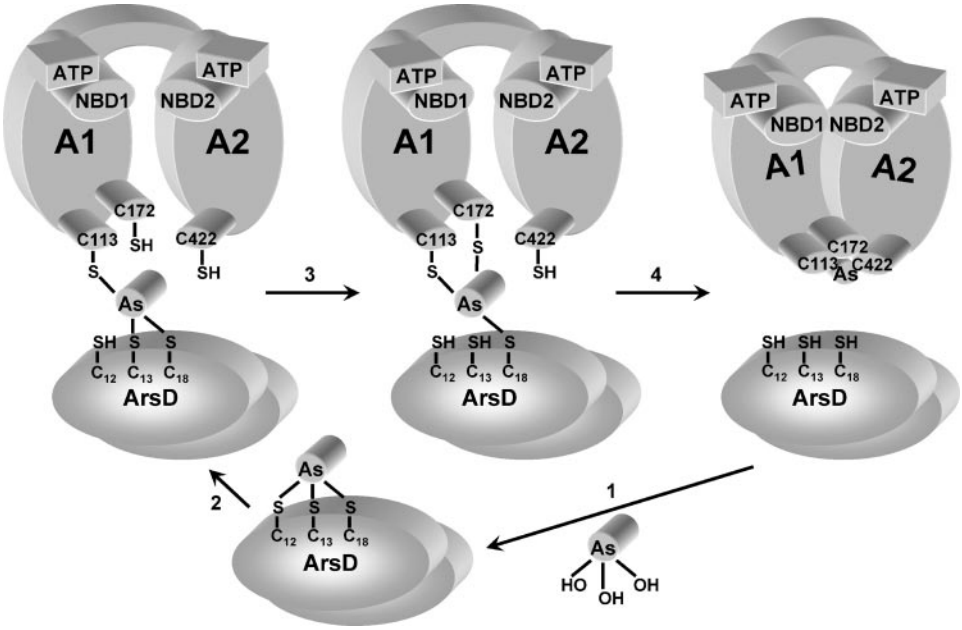

FIGURE 7. **Proposed mechanism of arsenic transfer between ArsD and ArsA.** *Step 1*, ArsD binds As(III) by exchange of the three hydroxyls of $As(OH)_3$ for the thiols of MBS1 residues Cys^{12}, Cys^{13}, and Cys^{18}. For simplicity, the cysteine residues of MBS1 are shown on only one subunit of the ArsD dimer. *Step 2*, exchange of one thiol ligand in MBS1 of ArsD for one thiol ligand in MBS1 of ArsA. *Step 3*, As(III) exchanges a second thiol ligand in ArsD for a second in ArsA. *Step 4*, As(III) is transferred to MBS1 in ArsA by a final ligand exchange, inducing a conformational change in ArsA that increases the rate of ATP hydrolysis. The model should not be taken to specify an order of ligand exchange in the transfer reaction.

measured. Wild type ArsD binds three metalloid atoms per monomer (or six per dimer). Elimination of any of the three vicinal cysteine pairs, Cys^{12}-Cys^{13}, Cys^{112}-Cys^{113}, or Cys^{119}-Cys^{120}, in turn, by mutagenesis or deletion, eliminated MBS1, MBS2, or MBS3, respectively, and a derivative having none of the cysteine pairs bound no metalloid. A cysteine-to-alanine substitution of Cys^{18}, which is conserved in all ArsD homologues identified to date, eliminated binding at MBS1, indicating that MBS1 requires Cys^{18} in addition to Cys^{12} and Cys^{13}.

MBS3 is not well conserved in ArsD homologues, and no phenotype has been associated with deletion of the C-terminal region containing MBS3. MBS2 has been associated with the weak transcriptional activity of ArsD (27), but substitutions or deletions of the cysteines in MBS2 do not eliminate the metallochaperone activity of ArsD. In contrast, MBS1 appear to be required for metallochaperone activity.

ArsD interacts with ArsA, the catalytic subunit of the ArsAB As(III)-translocating ATPase (4). ArsA is a pseudodimer, with two homologous halves, A1 and A2, each of which contains a nucleotide-binding domain (29). ArsA ATPase activity is activated by binding of As(III) or Sb(III) (23). In the structure three metalloid-binding sites are observed that are formed from residues contributed from both halves at the A1–A2 interface (29). Each metalloid is coordinated with one residue in A1 and another in A2, forming a "molecular glue" that brings the two halves of ArsA into contact with each other. Because each nucleotide-binding domain has residues from the opposite half of the protein, the formation of this A1–A2 interface is proposed to complete the nucleotide-binding domains, activating catalysis (30). Although Sb(III) is observed in all three ArsA MBSs in the crystal structure, only MBS1, containing Cys^{113} and Cys^{422}, is a high affinity binding site; the other two may be low affinity sites (31). Although Sb(III) is bound between Cys^{113} and Cys^{422} in the crystal structure, Cys^{422} is actually closer to Cys^{172} than Cys^{113}, and recent data suggest that Cys^{172} can participate in MBS1 at some point during the reaction.[3] Thus, we now consider ArsA MBS1 to be an S_3 site consisting of those three thiolates.

Although the details of metalloid transfer from ArsD to ArsA are presently unknown, the mechanism of copper transfer from copper chaperones to their respective partner proteins is instructive. Pufahl *et al.* (13) first proposed a chemical exchange reaction from transfer of copper from the yeast chaperone Atx1p to the N-terminal domain of the Cu(I)-translocating P-type ATPase Ccc2p. In this transfer, Cu(I) is initially two-coordinately bound to the two cysteine thiolates of the MT*CXXC* domain in Atx1p. It forms a transient three-coordinate complex with one of the cysteine thiolates of one of the MT*CXXC* domains of Ccc2p, followed by exchange of the Cu(I) from one of the thiolates in Atx1p to the second thiolate in the Ccc2p domain. This three-coordinate complex then dissociates to form free Atx1p and two-coordinately bound Ccc2p-Cu(I). Similar mechanisms have been proposed for the transfer of human Hah1 copper chaperone and the Menkes and Wilson disease proteins (32) and the yeast CCS chaperone and its partner superoxide dismutase (33). In the structure Hah1 is observed as a crystallographic dimer in which Cu(I) is bound four-coordinately to the two MT*CXXC* cysteine residues. This suggests that Hah1 and its yeast homologue Atx1p form heterodimers with the N-terminal domains of their respective copper pump partners and that transfer would occur by chemical exchange at their interfaces. Docking analysis of Atx1p and Ccc2p supports this mechanism (34). Similarly, the yeast CCS forms a heterodimer with superoxide dismutase and is proposed to use a similar chemical exchange mechanism between cysteine thiolates in the two proteins (33).

By analogy with the copper chaperones, we propose a hypothetical model of chemical exchange of As(III) between MBS1 in ArsD and MBS1 in ArsA (Fig. 7). Because ArsD and ArsA can be cross-linked with dibromobimane (4), it seems reasonable to propose that two proteins interact at their metalloid-binding sites. Although the details of the interaction are not known at this point, the yeast two-hybrid assays with C-terminal ArsD truncations show that the last 77 residues in ArsD are not required for interaction with ArsA. In contrast, two-hybrid

[3] X. Ruan, H. Bhattacharjee, and B. P. Rosen, manuscript in preparation.

analysis with N-terminal truncations suggests that a core region in ArsD from residues 5–43, including MBS1, is involved in both dimerization and interaction with ArsA. Metalloid bound to MBS1 in ArsD is transferred to MBS1 in ArsA, which is then extruded out of the cell by ArsB. Although not shown in the model, it is possible that ArsA MBS2 and MBS3 participate in sequential transfer of metalloid to ArsB. Even though the two monomers can be cross-linked to some degree with dibromobimane, it is not clear whether ArsD MBS1 is composed of cysteines from a single subunit or is formed intermolecularly. For that reason, the model shows only one monomer of ArsD. ArsA is shown in the ATP-bound form because nucleotide is required for metalloid transfer from ArsD to ArsA (4). The model implies that the chemical exchange occurs in three discrete steps, although the order is not known. The model provides a basis for future experiments.

REFERENCES

1. Abernathy, C. O., Thomas, D. J., and Calderon, R. L. (2003) *J. Nutr.* **133,** (Suppl. 1) 1536S–1538S
2. Beane Freeman, L. E., Dennis, L. K., Lynch, C. F., Thorne, P. S., and Just, C. L. (2004) *Am. J. Epidemiol.* **160,** 679–687
3. Rosen, B. P. (2002) *FEBS Lett.* **529,** 86–92
4. Lin, Y. F., Walmsley, A. R., and Rosen, B. P. (2006) *Proc. Natl. Acad. Sci. U. S. A.* **103,** 15617–15622
5. Bhattacharjee, H., Li, J., Ksenzenko, M. Y., and Rosen, B. P. (1995) *J. Biol. Chem.* **270,** 11245–11250
6. Wu, J., and Rosen, B. P. (1993) *Mol. Microbiol.* **8,** 615–623
7. Chen, Y., and Rosen, B. P. (1997) *J. Biol. Chem.* **272,** 14257–14262
8. Rosenzweig, A. C. (2002) *Chem. Biol.* **9,** 673–677
9. Eisses, J. F., Stasser, J. P., Ralle, M., Kaplan, J. H., and Blackburn, N. J. (2000) *Biochemistry* **39,** 7337–7342
10. Lin, S. J., Pufahl, R. A., Dancis, A., O'Halloran, T. V., and Culotta, V. C. (1997) *J. Biol. Chem.* **272,** 9215–9220
11. Walker, J. M., Tsivkovskii, R., and Lutsenko, S. (2002) *J. Biol. Chem.* **277,** 27953–27959
12. Rosenzweig, A. C. (2001) *Acc. Chem. Res.* **34,** 119–128
13. Pufahl, R. A., Singer, C. P., Peariso, K. L., Lin, S. J., Schmidt, P. J., Fahrni, C. J., Culotta, V. C., Penner-Hahn, J. E., and O'Halloran, T. V. (1997) *Science* **278,** 853–856
14. Cobine, P. A., George, G. N., Jones, C. E., Wickramasinghe, W. A., Solioz, M., and Dameron, C. T. (2002) *Biochemistry* **41,** 5822–5829
15. Wimmer, R., Herrmann, T., Solioz, M., and Wuthrich, K. (1999) *J. Biol. Chem.* **274,** 22597–22603
16. Sambrook, J., Fritsch, E. F., and Maniatis, T. (1989) *Molecular Cloning: A Laboratory Manual*, Cold Spring Harbor Laboratory, Cold Spring Harbor, NY
17. Adams, A., Gottschling, D. E., Kaiser, C., and Stearns, T. (1998) *Methods in Yeast Genetics: A Cold Spring Harbor Laboratory Course Manual*, Cold Spring Harbor Laboratory, Cold Spring Harbor, NY
18. Bhattacharjee, H., and Rosen, B. P. (2000) *Biometals* **13,** 281–288
19. Bradford, M. M. (1976) *Anal. Biochem.* **72,** 248–254
20. Gill, S. C., and von Hippel, P. H. (1989) *Anal. Biochem.* **182,** 319–326
21. Bhattacharjee, H., and Rosen, B. P. (1996) *J. Biol. Chem.* **271,** 24465–24470
22. Vogel, G., and Steinhart, R. (1976) *Biochemistry* **15,** 208–216
23. Hsu, C. M., and Rosen, B. P. (1989) *J. Biol. Chem.* **264,** 17349–17354
24. Fields, S., and Song, O. (1989) *Nature* **340,** 245–246
25. Rosen, B. P., and Borbolla, M. G. (1984) *Biochem. Biophys. Res. Commun.* **124,** 760–765
26. Dey, S., and Rosen, B. P. (1995) *J. Bacteriol.* **177,** 385–389
27. Li, S., Chen, Y., and Rosen, B. P. (2001) *Mol. Microbiol.* **41,** 687–696
28. Li, S., Rosen, B. P., Borges-Walmsley, M. I., and Walmsley, A. R. (2002) *J. Biol. Chem.* **277,** 25992–26002
29. Zhou, T., Radaev, S., Rosen, B. P., and Gatti, D. L. (2000) *EMBO J.* **19,** 1–8
30. Li, J., and Rosen, B. P. (2000) *Mol. Microbiol.* **35,** 361–367
31. Ruan, X., Bhattacharjee, H., and Rosen, B. P. (2006) *J. Biol. Chem.* **281,** 9925–9934
32. Wernimont, A. K., Huffman, D. L., Lamb, A. L., O'Halloran, T. V., and Rosenzweig, A. C. (2000) *Nat. Struct. Biol.* **7,** 766–771
33. Lamb, A. L., Torres, A. S., O'Halloran, T. V., and Rosenzweig, A. C. (2001) *Nat. Struct. Biol.* **8,** 751–755
34. Arnesano, F., Banci, L., Bertini, I., and Bonvin, A. M. (2004) *Structure* **12,** 669–676
35. Carlin, A., Shi, W., Dey, S., and Rosen, B. P. (1995) *J. Bacteriol.* **177,** 981–986
36. Chang, A. C., and Cohen, S. N. (1978) *J. Bacteriol.* **134,** 1141–1156